Journal of Oleo Science
Copyright ©2022 by Japan Oil Chemists' Society
doi : 10.5650/jos.ess21318
J. Oleo Sci. **71**, *(5) 671-683 (2022)*

Optimization and Characterization of *Cuscuta reflexa* Extract Loaded Phytosomes by the Box-Behnken Design to Improve the Oral Bioavailability

Saad M. Alshahrani*

Department of Pharmaceutics, College of Pharmacy Prince Sattam Bin Abdulaziz University, Al-Kharj, Kingdom of SAUDI ARABIA

Abstract: The purpose of this study is to determine whether the complexing hydroalcoholic extract of *Cuscuta reflexa* (HECR) with phosphatidyl choline increases its bioavailability. As a result, a novel phytosomal delivery system for the HECR-soya lecithin complex was developed (HECR-phytosome). The HECR-phytosome complex was synthesized and characterized as phytovesicles. The formulation was prepared using a variable concentration of soya lecithin (1:1–1:3 percent w/v), a temperature range of (45-65°C), and sonication time (4-8 min). Optimization of HECR-loaded phytosomal formulations was performed using Design Expert software. A three-factor, three-level Box-Behnken design was used to optimize this HECR delivery system, as dependent variables, vesicular size and entrapment efficiency were evaluated using a Box Behnken factorial design. Further characterization of the optimized formulation included vesicle size, PDI, zeta potential, entrapment efficiency, FTIR, DSC, TEM, and *in vitro* release. Vesicle sizes ranged from 173.5±6.17 nm to 215.9±6.53 nm, and response rates for entrapment efficiency ranged from 52.9±1.65 to 77.2±1.1%. The uniform structure and spherical shape were demonstrated by transmission electron microscopy. Among the drug release kinetic models, the formulation followed the Higuchi model (R^2 = 0.9978), releasing 96.3±3.7% of the polyphenol and flavonoids phytoconstituents from HECR-loaded phytosomes in 12 hours, compared to 49.3±2.5% in the plain extract. In addition, the optimized formulation passes the stability test. Therefore, the results demonstrated that phytosomal nanocarriers have the potential to increase the bioavailability of *Cuscuta reflexa* extract.

Key words: *Cuscuta reflexa*, phytosomes, Box Behnken design, bioavailability, polyphenol

1 Introduction

Recent literature findings have shown bioactive compounds utilized in current therapies have natural origins for the vast majority of the time, according to recent literature studies. This means that they are obtained from natural items or their chemical structure was inspired by natural goods for the most part[1]. *Cuscuta reflexa*, a member of the Convolvulaceae family, is one such therapeutic plant. According to previous studies, the antioxidant, antibacterial, antispasmodic, hemodynamic, antihypertensive, antidiabetic, hepatoprotective properties of *Cuscuta reflexa* have been demonstrated[2–4]. Also, from this herb, a wide range of bioactive constituents have been isolated; among them are kaempferol, astragalin, myricetin, quercetin, and sesamin. Other bioactive constituents found in this herb include isorhamnetol, linoleic and/or oleic acids, stearic and/or palmitic acids, luteolin, and sesamin[5–8]. Among the most potent antioxidant molecules are flavonoids including kaempferol, astragalin, myricetin, quercetin, and isorhamnetol. Reactive oxygen species cause oxidative damage, which quercetin may help to reduce. Notably, this has aided in keeping low-density lipoprotein oxidation at bay, preserving beta-pancreatic cell function, as well as preventing cardiovascular diseases like cancer and diabetes mellitus from progressing as quickly, as well as protecting cells from oxidative stress caused by chronic alcohol consumption[1, 9, 10].

Oral quercetin usage reveals relatively poor absorption by the intestinal membrane because of the hydrophilic nature of quercetin. This is attributed to the polyphenol structure's numerous OH groups, which make it too polar to pass through the intestinal lipid membrane and the molecule's inherent instability in various physiological fluids. The list of substrates for these multidrug resistance-associ-

*Correspondence to: Saad M. Alshahrani, Department of Pharmaceutics, College of Pharmacy, Prince Sattam Bin Abdulaziz University, Al-kharj, SAUDI ARABIA
E-mail: sm.alshahrani@psau.edu.sa
Accepted January 25, 2022 (received for review October 18, 2021)
Journal of Oleo Science ISSN 1345-8957 print / ISSN 1347-3352 online
http://www.jstage.jst.go.jp/browse/jos/ http://mc.manusriptcentral.com/jjocs

ated proteins (MRP) includes plant polyphenols, resveratrol, and quercetin. MRP is an efflux transporter that is ATP-dependent. To make quercetin less bioavailable, MRP removes the compound from the intestinal lumen, where it cannot enter the bloodstream[11, 12]. If quercetin is consumed orally, it is degraded into phenolic acids (such as protocatechuic acid) with limited stomach absorption at low pH and extensive intestinal and hepatic Glucuronidation, sulfuration, and methoxylation before being converted back to quercetin by enzymatic means. This process is known as the metabolic degradation of quercetin. As a result, a significant number of metabolites are generated, including quercetin-3-O-d-glucuronide (Q3GA), the main quercetin metabolite that circulates in the bloodstream[12, 13].

Phytosomes, a lipid-like carrier, can be used to formulate *Cuscuta reflexa* extract and solve the absorption and bioavailability issues with quercetin. These fat-soluble complexes are created by combining plant extracts with phospholipids in nanovesicles, which are known as phytosomes. The *Cuscuta reflexa* extract's medicinal efficiency can be enhanced by using phytosomes, which are also transporters[14] phytosomes are more absorbable through the intestinal lipid membrane than herbal extracts. A potential method for optimizing the pharmacological activity of plant extracts after oral administration and improving their safety has been generally accepted the encapsulation of the extract in nanosystems[15, 16].

A novel formulation of *Cuscuta reflexa* extract was designed and developed using a phytosome delivery method. There are no unbound active molecules in a phytosome, which means that any water-soluble phytoconstituents that are present in the extract are absorbed into the phospholipids[17]. The phytosome releases hydrophilic quercetin into an enterocyte membrane's lipid environment, allowing it to enter the circulation. Results from this study indicated that incorporating quercetin into phytosomes enhanced its intestinal permeability, which improved its bioavailability in humans significantly. Human pharmacokinetic studies have shown that giving quercetin phytosome instead of quercetin alone increased absorption, AUC, and C_{max} significantly. And no significant adverse effects were detected from the quercetin phytosome therapy[18]. There are several well-known herbal extracts including hawthorn, Ginkgo biloba, milk thistle, ginseng, green tea, and grape seed that have been given phytosome treatment as a trend in herbal medicine and nutraceutical delivery.

In other words, phytosome is an entirely new, patent-pending method of incorporating hydrophilic phytoconstituents or standardized plant extracts into the phospholipids to produce lipid-compatible molecules with greater bioavailability than conventional herbal extracts thus they have a greater potential to penetrate the lipoidal biomembrane and subsequently enter the systemic circulation[19].

Advanced, high-performing and standardized *Cuscuta reflexa* extract phospholipid complexes were used in this study to improve the efficacy and safety of the *Cuscuta reflexa* plant extract. Variations in extract/phospholipid (w/w) ratios were used to incorporate the whole extract into phytosomes, and the Box Behnken Design was used to change the desirability function for 3-factors and 3-levels[20]. Independent variables (factors) were the amount of soya lecithin and *Cuscuta reflexa* extract (X1), temperature (X2) and sonication time (X3) for two dependent variables i.e. vesicle size (Y1) and entrapment efficiency (Y2). Seventeen batches of the quadratic response surfaces were prepared and then analyzed to identify the best conditions for exploration. Thus, the rationale of proposed study was to fabricated *Cuscuta reflexa* phytosomes, to enhance the bioavailability of prepared formulation.

2 Materials and Methods

2.1 Extraction of plant material

To extract the drug, the aerial part of *Cuscuta reflexa* were shade dried and coarsely pulverized, then packed in a Soxhlet apparatus (EIE - 213EP, Ellis Bridge, Ahmedabad, India). Further it was extracted with petroleum ether (60-80℃) for 24 hours to remove the fat from the plant material[21]. After that, the exhausted drugs were extracted with the hydroalcoholic solvent [ethanol:water (60:40) (Fig. 1)]. The hydroalcoholic extract of *Cuscuta reflexa* (HECR) was made by evaporating the solvent traces in a rotary evaporator (RE5002, Rotary Evaporator, Chemical Industry, Zhengzhou, China) until a powdered mass was formed, and the crude extract was preserved in an airtight container for further investigation.

2.2 Determination and quantification of quercetin by HPLC

The sample extracts were measured using HPLC. The separation was carried out on a 4.6×250 mm analytical C18 column[22]. The flow rate was set to 1 mL/min in this scenario. In the isocratic mode, 0.1 percent formic acid in water (solvent A) and 100 percent acetonitrile (solvent B) were employed to make the mobile phase, with a final pH adjustment of 6.8. The following elution gradients were employed to achieve this: 0-50 min at 30% B and 51-60 min at 50% B. The injection volume was set at 20 μL. At a wavelength of 280 nm, the fingerprint profiles were recorded. The quantity of quercetin was determined using peak area measurements.

2.3 Preparation of HECR phytosomes

The HECR phytosomes complex was prepared utilizing the technique of Upadhyay *et al.* with slight modification[23]. Briefly, the amount of *Cuscuta reflexa* and soya lecithin was added in a molar ratio to prepare the complex in the

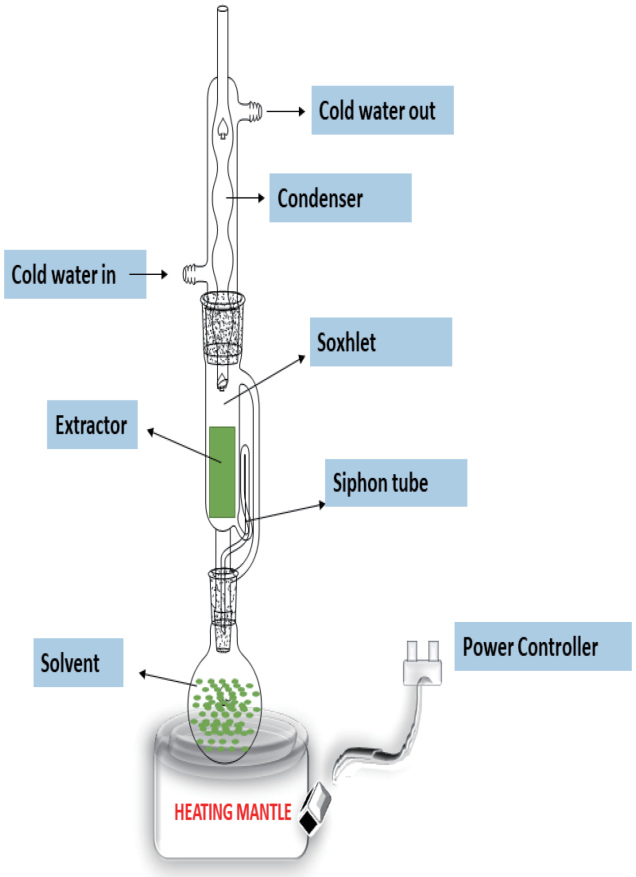

Fig. 1 Preparation of hydroalcoholic extract of *Cuscuta reflexa* (HECR) using Soxhlet apparatus.

ratio of 1:1, 1:2, and 1:3. In a 100 mL round-bottom flask, a weight quantity of extract and soya lecithin were poured, and 20 mL of acetone was poured as a reaction medium. For 3 hours, the mixture was refluxed and the complex's reaction temperature was adjusted to 50℃. Approximately 20 mL of *n*-hexane was added to the clear liquid after it had been evaporated with constant stirring. In order to eliminate the remaining solvents, the precipitate was filtered and vacuum-dried. The dried residues were collected and kept in amber-colored glass bottles at room temperature after being desiccated overnight (Fig. 2).

2.4 Experimental design

To optimize the formulations Box-Behnken design of the experiment (trial version 13.0.2.0, Stat Ease Inc. Minneapolis, USA) was employed, which is a response surface type design of experiment, whereby responses of three components were investigated at three levels[24]. Independent factors such as soya lecithin and *Cuscuta reflexa* (X1); temperature (X2); and sonication duration (C) at three levels; low, medium, and high i.e. (−1, 0, +1) as indicated in the preliminary risk assessment (Table 1). A total of three replicates of each experiment were used, with the average of each value being used for further analysis. There was a total of 17 experiments, each with five different centers point in each block. These independent variables (X1, X2, and X3) were examined for their impact on dependent variables Vesicle size (Y1), and Entrapment efficiency (Y2) by building two- and three-dimensional (2-D and 3-D) models of their response surfaces, as well as quadratic equations, with the aid of Design Expert software. Soya lecithin and *Cuscuta reflexa*, temperature, and sonication time were all tweaked to perfection. The screening was designed using a BBD to help reduce the number of trials while still getting the most information possible on the product's characteristics. For the study of the interaction effect of two factors on reaction at the same time concurrently, the terms X1, X2, X3 and their combination (X1X2, X1X3, X2X3 and square value (X12, X22, X32) were used.

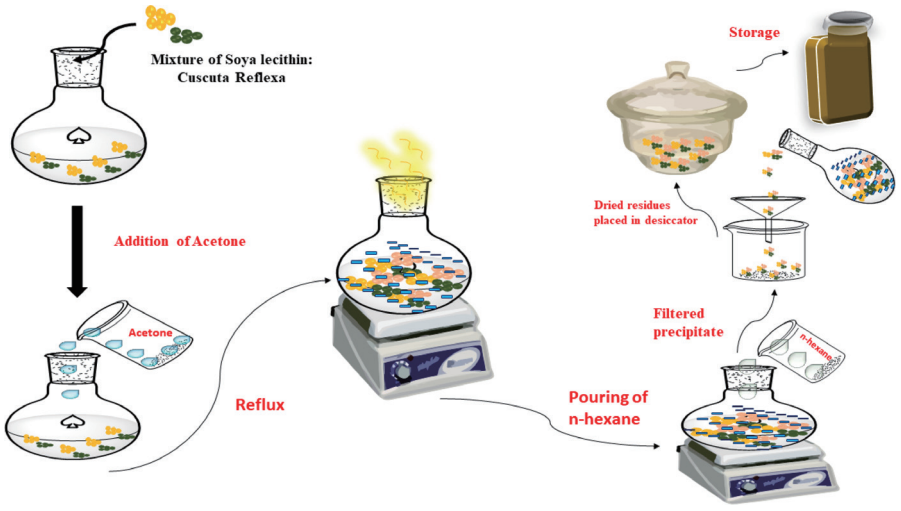

Fig. 2 Formulation steps for HECR phytosomes.

Table 1 Details of Box-Behnken Design coded and actual values for phytosomes formulation.

Independent variables	Units	Coded Value		
		Low (–1)	Medium (0)	High (+1)
Amount of soya lecithin: Cuscuta reflexa extract (X1)	molar ratio	1:1	1:2	1:3
Temperature range (X2)	℃	45	55	65
Sonication time (X3)	min	4	6	8
Dependent variables	Units		constraints	
Particle size (Y1)	nm		Minimum	
Entrapment efficiency (Y2)	%		Maximum	

2.5 Characterization of *Cuscuta reflexa* loaded phytosomes

2.5.1 Determination of vesicle size, PDI and Zeta potential of HECR phytosomes

The vesicle size and PDI evaluated the principle of dynamic light scattering by zeta sizer (Malvern Zeta master ZEM 5002, Malvern, UK)[25]. Distilled water was used as a solvent for dilution of the sample and placed in a quartz cuvette at a 90° scattering angle. All the batches were analyzed in a triplicate manner, and the mean and SD were calculated.

2.5.2 Entrapment efficiency of HECR phytosomes

HPLC was used to measure the entrapment efficiency (EE), which represents the quantity of quercetin integrated into phytosomes. The centrifugation method was used to assess phytosomal vesicles entrapment effectiveness. To separate the flavonoids (quercetin) that were not entrapped in the supernatant, the clear supernatant was separated. A high-speed cooling centrifuge (REMI ultra-centrifugation) was used to separate the vesicles at 12,000 rpm for 60 minutes at 4℃[26]. Sediment was treated with 1 mL of 0.1% Triton X 100 to lyse the vesicles and appropriate dilution was made with phosphate buffer saline (pH 7.4) to measure the quercetin content using HPLC. The absorbance of the supernatant for non-entrapped HECR phytosome at λ_{max} 280 nm was measured using HPLC.

The % EE was determined by the following formula:

$$\% \text{ EE} = (\text{Amount of drug added} - \text{Amount of free drug}) / (\text{Total amount of drug added}) \times 100$$

2.5.3 Morphological examination

2.5.3.1 Transmission electron microscopy

The vesicular shape of developed phytosomes was examined using transmission electron microscopy (TEM, Hitachi, H-7500 Tokyo, Japan). To examine nanomaterial crystallization and dispersion, as well as to measure vesicle size, a transmission electron microscope (TEM) was employed. TEM is a microscopy method that transmits an electron beam through an ultra-thin specimen, interfacing with the specimen as it goes through. As the electrons pass through the specimen, an image is created. This picture is amplified, then focused on an imaging device such as a fluorescent screen, photographic film, or a sensor like a CCD camera. On a carbon-coated grid, the sample was collected and phosphotungstic acid was used to stain it. At a voltage of 200 kV, 10–100k times enlargements were detected under a microscope[27].

2.5.4 Drug excipient study by FTIR

The interaction between HECR and optimized HECR-phytosomes was studied using FTIR analysis, which uses a Fourier-transform infrared spectrum. A 1% w/w of the sample with KBR was triturated to a fine powder and then crushed for 30 seconds in a hydraulic press at 10,000 psi. With the use of an FTIR spectrophotometer, the spectra were analyzed in the 4000–400 cm-1 range (Nicolet IZ 10, Thermo Fisher Scientific, Waltham, MA, USA)[28].

2.5.5 Drug excipient study by DSC

The HECR extract and HECR loaded phytosomes were subjected to DSC using a differential scanning calorimeter (DSC 200 F3, Netzsch, German). A conventional aluminum pan was used to encapsulate the samples, and they were heated in a nitrogen environment at a rate of 10℃/min from 40℃ to 250℃. For the analysis, a blank aluminum pan served as a reference. An analyzer was used to find the peak transition start temperature, and the results from each sample were compared[29].

2.5.6 *In vitro* release studies

The *in vitro* release pattern of plain HECR solution and HECR loaded phytosomes was measured using the dialysis approach. An appropriate amount of phytosomal formulation (HECR content 1 mg/mL) was deposited on a dialysis membrane in a beaker containing 200 mL of 0.1 N HCL (pH 1.0) and heated to 37 ± 0.5℃ with continuous stirring at 75 rpm to maintain the temperature[30]. At varied time intervals (1 hr, 2 hr, 4 hr, 6 hr, 8 hr, 10 hr and 12 hr), the aliquots (2 mL) were withdrawn and replaced with 0.1 N HCl (pH 1.0). For the determination of quercetin quantity in HECR phytosomes, withdrawn samples were filtered

through Whatmann filter paper and analyzed by HPLC at 280 nm. The procedure was carried out three times. In order to explain the release profile of a pharmaceutical in various formulations, it is critical to guarantee that drug dissolution occurs properly. Different kinetic models were used to characterize the drug release profile from the phytosomal formulation in terms of the amount of drug released as a function of the test time. The *in vitro* release kinetics data of an optimized HECR phytosomal formulation was examined concerning zero order, first order, Higuchi model, and Korsemayer peppas plot by plotting graphs for all of the following models.

2.6 Stability studies

Stability experiments were carried out to determine the requisite physical stability of the optimized nano formulation at high storage temperatures and relative humidity. The improved phytosomal formulation's entrapment efficiency, particle size change, and physical appearance were all evaluated in a stability study. For three months, the formulations were kept at 4 ± 0.5℃ in glass containers[31]. The samples were taken in triplicate at 0 days, 1 month, 2 months, and 3 months. Weiss Technik North America's CSZ Stable Climate® II stability chamber was used to conduct the investigation. The samples were kept under observation, and physical changes such as particle size and drug entrapment efficiency (%) were assessed at regular intervals.

3 Results and Discussions

3.1 Quantification of polyphenolic compound

The concentration of polyphenol such as quercetin in the *Cuscuta reflexa* was determined using the HPLC technique[32]. To accomplish the analysis, the HPLC was run for 50 minutes. The presence of quercetin was shown by the retention duration of 46.1 minutes, indicating that the HPLC approach utilized in this work may enable convenient and rapid detection of quercetin, which researchers demand. The standard concentrations of quercetin and chromatograms showed good linearity. It has been found that the mobile phase gradient elution profile was most effective in practically all studies. In the current work, however, a simple isocratic elution was used, making quercetin detection easier and faster. After 46.1 minutes, the quercetin peak appeared. The area acquired from the analysis was then calculated into the calibration curve, yielding a quercetin concentration of 52.19 percent in the extract. The HECR contained an abundant quantity of quercetin and showed potent antioxidant activity, which protects against oxidative stress damage, which is linked to a variety of disorders. The oral bioavailability of quercetin is poor due to its hydrophilic nature and larger molecular weight. The encapsulation of HECR into phytosome formulation can improve the absorption rate, solubilization extent in aqueous intestinal fluids as well as capacity to traverse biomembranes. Further, the activity of these types of phytosomes has been extensively documented in a variety domain of applications such as hepatoprotective, cardiovascular, anticancer, anti-inflammatory, and many more[1].

3.2 Preparation and optimization of HECR loaded phytosomes

Soya lecithin and HECR were combined with organic solvents acetone and *n*-hexane to create phytosomes. Different formulation variables, such as soya lecithin content, temperature, and sonication time, were selected as independent factors for optimization utilizing Design Expert software based on preliminary research. As stated in Table 2, the lecithin concentration was set to 1:1–1:3 (molar ratio), the temperature was set to 45–65℃, and the sonication time was set to 4–8 minutes (min). Design Expert software was used to analyze the observed results of independent variables across all 17 formulations. The three-factor three levels box Behnken design with 5 center points (0, 0, 0) was used in the study. To avoid any error, and achieve more accuracy for the formulation, five center points were investigated. In the case of 15 batches, other researchers take three center points (Marasini *et al.* 2012)[33]. Whereas, Rathee *et al.* 2017 prepared 17 batches with five center points[34]. Similar to Rathee *et al.* we also prepared 17 batches comprising of three-level three-factor box Behnken design with five center points.

3.3 Analysis of optimization data of HECR loaded phytosomes

Results showed that the different combinations of variables have a significant effect on the responses of dependent variables viz. particle size (Y1), and entrapment efficiency (Y2), which were shown in (Table 2). Vesicle sizes ranged from 173.5 ± 6.17 nm to 215.9 ± 6.53 nm, while entrapment efficiency response rates ranged from 52.9 ± 1.65 to 77.2 ± 1.1.

The relationship between independent factors and vesicular size is described by the following coded equation 1:

$$\text{Vesicle Size (Y1)} = +181.34 + 6.10X1 + 4.76X2 + 5.91X3 + 4.45X1X2 + 4.65X1X3 + 6.78X2X3 + 7.49X1^2 + 1.62X2^2 + 12.87X3^2 \quad \text{Eq. 1}$$

The equation reveals that component A (soya lecithin concentration) has a positive effect on the vesicular size, while factor B (temperature) has a positive effect. The higher-order terms (A2 and B2), as well as the interaction terms (AB), had a beneficial effect on vesicular size. As a result, increasing the amount of soya lecithin and *Cuscuta reflexa* from a low to an intermediate level causes vesicle size to increase. Increasing soya lecithin concentration

Table 2 Response values of experimental runs; Amount of soya lecithin: *Cuscuta reflexa* (X1), temperature (X2), sonication time (X3) [Values are expressed as mean ± SD, (n = 3)].

Formulation code	CQAs			CMAs	
	X1	X2	X3	Y1 (Vesicle size, nm)	Y2 (Entrapment efficiency, %)
HECR1	−1	−1	0	177.5 ± 6.17	58.5 ± 2.53
HECR2	0	0	0	187.1 ± 8.11	62.3 ± 2.2
HECR3	0	−1	1	208 ± 7.37	67 ± 3.61
HECR4	0	0	0	184.7 ± 4.83	61.3 ± 5.75
HECR5	0	−1	−1	179.1 ± 6.51	71.6 ± 1.1
HECR6	0	1	−1	213.7 ± 6.57	52.9 ± 1.65
HECR7	1	0	1	214.6 ± 8.89	77.2 ± 1.1
HECR8	−1	0	1	181 ± 6.21	67.3 ± 3.04
HECR9	0	0	0	193.5 ± 6.41	56.3 ± 4.25
HECR10	−1	1	0	186.7 ± 9.94	66.3 ± 1.56
HECR11	1	0	−1	215.9 ± 6.53	75.8 ± 2.78
HECR12	0	0	0	210.9 ± 7.31	75.5 ± 3.67
HECR13	0	1	1	192.7 ± 3.32	59.7 ± 3.52
HECR14	−1	0	−1	184.9 ± 8.37	54.1 ± 2.73
HECR15	1	−1	0	185.1 ± 8.24	68.1 ± 3.02
HECR16	0	0	0	173.5 ± 6.17	69.5 ± 2.53
HECR17	1	1	0	187.1 ± 8.11	62.3 ± 2.2

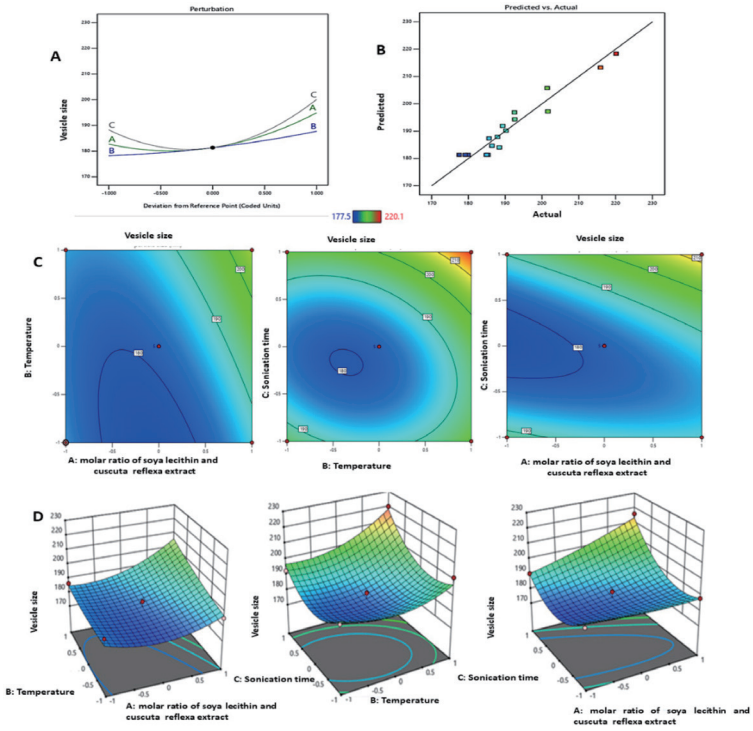

Fig. 3 Graphs of vesicle size models (A) Perturbation curve; (B) Linear correlation plot; (C) 2D contour plots; (D) 3D Response surface plots.

beyond this resulted in an increase in vesicle size. Although it has been discovered that the amount of lipid, sonication period, and temperature all have a direct relationship. The 2D and 3D plots of the response surface and contour plot in Fig. 3 show the fluctuations in vesicular size with lecithin concentration and rotation speed. The response surface plot shows that vesicular size grows as the concentration of lecithin increases, whereas vesicular size increases as the sonication time increase to a certain point, but vesicular size decreases at high speed. As the soya lecithin: *Cuscuta reflexa* molar ratio was raised, the size of the vesicles increased, which may be ascribed to the phytosomes' rising phospholipid content. For example, Dubey *et al.* found an association between Phospholipon (PL) percent and an anti-psoriatic agent-loaded ethosome vesicle size[35]. According to Ahmed *et al.*, when Phospholipon concentration increased, the size of avanafil invasome vesicles grew[36]. As a whole, our findings show better results as compared to the other reported evidence on vesicular systems.

The coded entrapment efficiency equation derived by Design Expert software is shown in equation 2.

$$EE(Y2) = +73.30 + 2.93X1 + 1.44X2 + 6.65X3 + 3.10X1X2 - 0.0525X1X3 + 2.52X2X3 - 4.80X1^2 - 4.80X2^2 - 8.42X3^2 \quad \text{Eq. 2}$$

Figure 4 shows the 2D and 3D plots, which show a favorable relationship between HECR entrapment efficiency with X1. When X1 was increased, greater entrapment efficiency was noticed as a result of the bigger drug/bioactive carrying capacity of lipid. The entrapment efficiency increased when the sonication time was increased. Collision or electrostatic interaction between vesicles is more probable due to physical interaction. As a result, larger vesicles result in more HECR extract entrapment. Although the temperature has a significant impact on the production of HECR phytosomes. As the temperature and sonication period is increased, the entrapment efficiency improves[37, 38].

3.4 Desirability optimization and checkpoint analysis

The goal of optimization was to discover the circumstances that result in the highest EE while maintaining the smallest vesicle size and PDI. To attain this purpose, a desirability function method was applied. Table 3 shows the constraints that were imposed in the software for this optimization. The formulation's ideal composition was determined utilizing the maximum desirability technique and the Design Expert's post-analysis point prediction capability. The desired target for critical quality attributes includes minimal particle size and maximum entrapment efficiency were used to create the intended objective (Table 3). Software suggested maximum desirability value of 0.73%

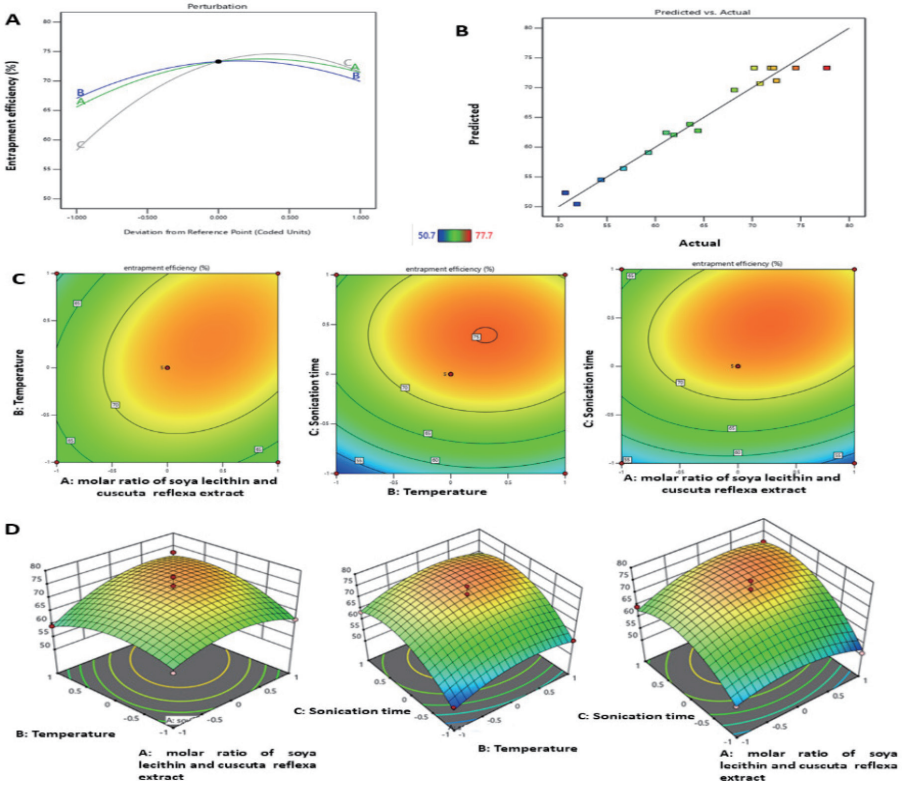

Fig. 4 Entrapment efficiency model graphs, (A) Perturbation curve; (B) Linear correlation plot; (C) 2D contour plots; w (D) 3D Response surface plots.

Table 3 Solutions obtained after post analysis point prediction using Design Expert.

Variables	Ratio of soya lecithin and cuscta reflexa (%)	Temperature (℃)	Sonication time (hr)	Vesicle size (nm)	Entrapment Efficiency (%)
Predicted results	0.073	0.52	0.27	192.5	69.4
Observed results				173.5 ± 6.17	77.2 ± 1.1
Percentage Prediction error (%)				5.17%	3.27%

having optimized formulation components i.e. ratio of soya lecithin and HECR (X1) = 0.073%, temperature (X2) = 0.52℃, and sonication time (X3) = 0.27 hr. On the other hand, checkpoint batches were compared to software-predicted responses (Table 3). The findings showed the predicted and observed vesicle size was 192.5 nm and 173.5 ± 6.17 nm respectively, with entrapment efficiency of 69.4 nm and 77.2 ± 1.1 respectively.

3.5 Vesicle size, PDI and zeta potential

The mean vesicle size of dispersed components in colloidal delivery systems affects their bioavailability, turbidity, and stability. Colloidal systems with a larger mean vesicle size exhibit more colloidal instability (gravitational separation) bioavailability, and turbidity than those with a smaller mean vesicle size. The amount of quercetin intercalated within the lipid membranes affects the nanoformulations' mean vesicle size, PDI, and zeta potential. All formulations had vesicle sizes ranging from 173.5 ± 6.17 nm to 215.9 ± 6.53 nm. The size of the vesicle tends to grow as the concentration of the complex increases. When particle concentrations are excessively high, physical interactions between vesicles, such as collisions or electrostatic interactions, become more prominent. These interactions cause the particles to travel differently and generate bigger vesicles. The high lipid content of the formulation also enhances the likelihood of agglomeration, resulting in larger vesicle sizes.

Most particles have a surface area/volume (SA/V) ratio inversely related to vesicle size. As a result, smaller vesicle sizes with a greater SA/V allow the encapsulated medication to be released from the phytosomes more easily via diffusion and surface erosion. They also allow the medication entrapped in the phytosomes to infiltrate and permeate past physiological drug barriers. Previously, LeFevre *et al.* found that lymphatics take up bigger particles (≤ 5 mm), but smaller particles (≤ 500 nm) may easily pass the epithelial cell membrane through endocytosis[39]. All of the developed formulae have polydispersity index values of less than 0.2. The polydispersity of phytosomes is examined in order to ascertain the size and distribution homogeneity of phytosomes. The PDI value for a monodisperse system must be less than 0.1, whereas the PDI value is more than or equal to 1.0, then the vesicles are extremely polydisperse and contain particles of various sizes. Lower PDI values indicate better particle size homogeneity. PDI of 0.3 or less is regarded as acceptable in drug delivery applications using lipid-based carriers, indicating greater phospholipid vesicle homogeneity[11, 40, 41]. The PDI achieved for formulations was less than 2, resulting in the most homogenous particle size distribution. This reflects the system's vesicle size consistency and homogeneity. The average ZP of the HECR phytosomes was −52.6 ± 5.8 mv. As the concentration of quercetin entrapped increases, the surface charge becomes more negative. Because strong electronegative values are typically indicative of stable nano formulations, these findings suggest that quercetin entrapment increases the physical stability of phytosomes. Compared to flavonosomes produced using other techniques, the zeta potential for the improved formulation was substantially more negatively charged −52.6 ± 5.8 mv. It indicates that the formulation has more than the average amount of the normal threshold levels for attraction and flocculation for repulsion. The presence of complexes explains the greater negative zeta potential of formed flavonosomes; it maintains the flavonosomes' dynamic stability in aqueous conditions. Thus, the improved formulation exhibited high zeta potential, tiny vesicle size, and narrow monodisperse size distribution (low polydispersity index value), indicating that the formed flavonosomes had outstanding stability.

In addition, it is the amount of the zeta potential that indicates the degree of electrostatic repulsion between contiguous, similarly charged particles dispersed in a solution. The presence of a strong zeta potential imparts stability on molecules and particles of suitable size. A colloidal dispersion may flocculate when the potential is low because the attracting forces dominate the repulsive forces. There must be a balance between the attractive van der Waals interactions between vesicles and electrical repulsion for phytosomes to be stable.

3.6 Entrapment efficiency

The effectiveness of entrapment is an essential metric for characterizing phytosomes. Several parameters were adjusted to achieve maximum encapsulation efficiency, including the amount of soya lecithin, the amount of HECR, and the amount of Acetone. The phytosome entrapment

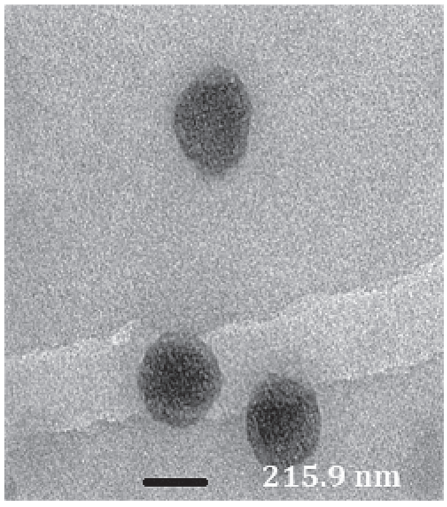

Fig. 5 TEM micrograph of optimized formulation (20000x magnification).

efficiency was determined to be between 52.9 ± 1.65 and 77.2 ± 1.1%. Considering the huge percentages of EE produced, the lipid/medication ratio used is the optimum option for HECR phytosome preparations. Because of the planar nature of quercetin, it may easily intercalate into the ordered structure of phosphatidyl choline inside membranes, preventing it from being released. The lipid composition of phytosome membrane components influences the efficacy of HECR entrapment. As a result, the amount of HECR incorporated into phytosomes is strongly reliant on phospholipid/HECR ratios. A vesicular system must include more phospholipids than typical to increase its ability to collect water-insoluble medications.

3.7 Vesicular shape determination

3.7.1 Transmission electron microscopy

TEM micrograph shown in Fig. 5, suggests the spherical shape of the phytosomal formulation. Also, the size depicted in the TEM micrograph of the optimized formulation was 173.5 and 215.9 nm, which was in correlation with the size observed in the zeta sizer.

3.8 FTIR analysis

The HECR's FT-IR spectra were obtained and expressed the presence of hydroxyl groups. The presence of major chemical groups in the obtained HECR supports the existence of flavonoids such as quercetin. The typical peaks of quercetin were found in 3371.23, 2852.41, 1700.06, 1152.2, and 1069.13 cm^{-1}. The intensity of the OH peak in HECR-loaded phytosomes was found to be lower when compared to crude HECR (Fig. 6). This demonstrates that a complex was created by the creation of hydrogen bonds between the extract and the lipid molecules. This interaction explains why quercetin has such a high loading value.

3.9 DSC analysis

To ensure the development of a complex between HECR and phospholipid, differential scanning calorimetry was used. Figure 7 shows DSC thermograms of HECR and HECR-loaded phytosomes. HECR's endothermic peak was detected at 62.9℃, which corresponded to its melting point. The main endothermic peak in the HECR phytosomes, on the other hand, was detected at 75.9℃ (Fig. 7). Thermograms of HECR phytosomes revealed the absence of HECR's endothermic melting peak, showing that HECR was entirely immersed into the matrix of phytosomes, which had different thermal characteristics than the HECR individual. Phosphatidylcholine and HECR interact via hydrogen bonding between the -OH group of HECR and the polar portion of phosphatidylcholine. Furthermore, the results revealed that the HECR is crystalline, which is the most stable form with a high melting point but may have limited solubility.

3.10 *In vitro* drug release study

After 12 hours, a comparative drug release pattern of HECR-loaded phytosomes and plain crude extract (HECR) were estimated using HPLC. The results showed that in the first two hours of drug release studies, plain extract solution and HECR loaded phytosomes followed a similar drug release pattern, but after that, HECR loaded phytosomes provided 96.3 ± 3.7 percent of the released. While plain extract solution provided 49.3 ± 2.5 percent release after

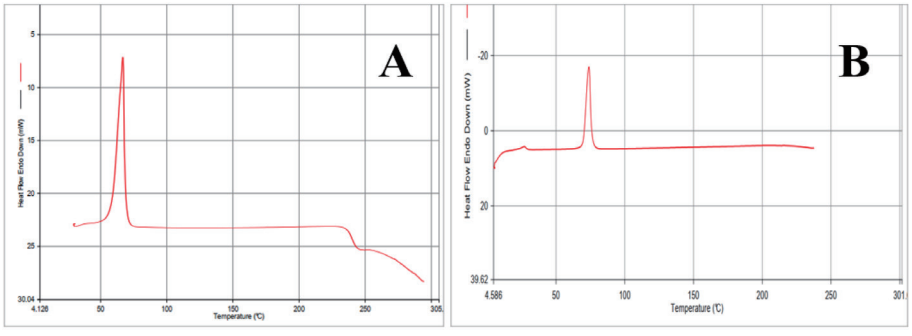

Fig. 6 A) FTIR Spectra of HECR; B) FTIR Spectra of HECR loaded phytosome.

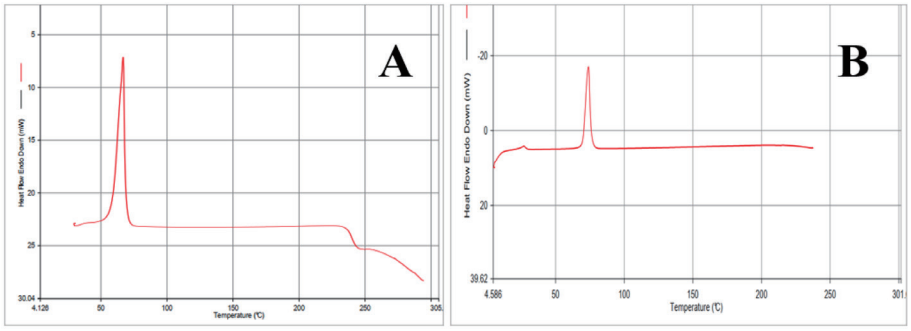

Fig. 7 A) HECR DSC Thermogram; B) HECR loaded phytosomes DSC Thermogram.

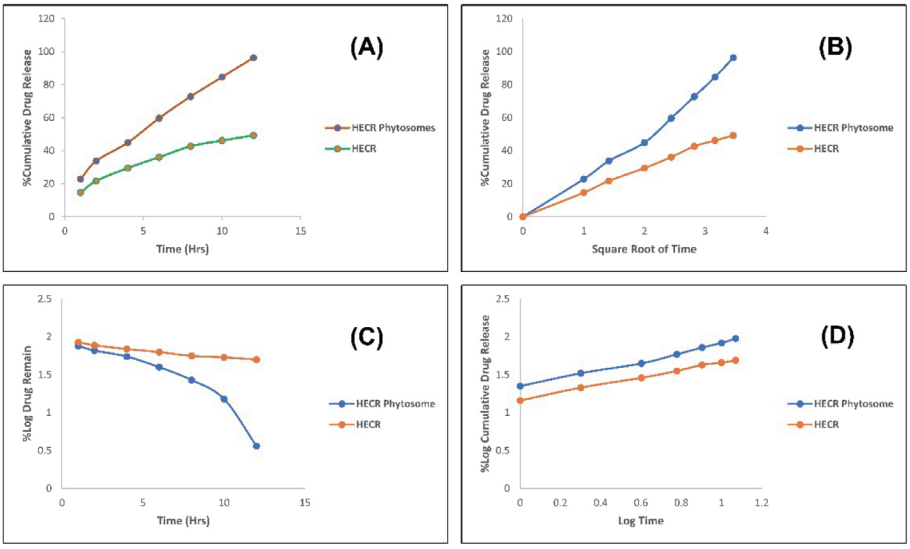

Fig. 8 Cumulative drug release and drug release kinetics profile of HECR and HECR loaded phytosomes (A) zero order; (B) Highuchi model; (C) First order; (D) Korsemayer peppas model.

Table 4 Data of drug release and kinetic of HECR and HECR loaded phytosomes.

Parameters	HECR	HECR loaded phytosomes
Release kinetics		
Correlation Coefficient (R^2)		
Zero Order Model	0.9608	0.9963
First Order Model	0.8742	0.9760
Higuchi Matrix Model	0.9978	0.9971
Korsemayer Peppas Model	0.9975 (n = 0.4951)	0.9924 (n = 0.5783)
Cumulative release after 12 h	49.3 ± 2.5	96.3 ± 3.7

12 hours (Fig. 8). It was demonstrated that HECR-loaded phytosomes release a high percentage of quercetin because their flexible bilayer structure allows quercetin contained in the aqueous layer of phytosomes to migrate outward, increasing its solubility and wettability. It was also discovered that the amphiphilic nature of cholesterol and phospholipids improved the profile of quercetin's low water solubility.

In vitro release kinetics pattern of the HECR solution and optimized HECR loaded phytosomes were studied by using the zero order, first order, Higuchi, and Korsemayer peppas models (Table 4). The R^2 values of zero order, first order, Higuchi, and Korsemayer peppas models of simple HECR solution are 0.9608, 0.8742, 0.9978, and 0.9975 (n = 0.4951), respectively. Furthermore, the R^2 values of zero

order, first order, Higuchi, and Korsemayer peppas models of HECR loaded phytosomes R^2 values are 0.9963, 0.9760, 0.9971, 0.9924 (n = 0.5783), respectively. The high correlation values for Higuchi's equation of plain extract solution and HECR loaded phytosomes, 0.9978 and 0.9971, respectively, indicate that diffusion is the mechanism of drug release. The drug release mechanism is defined by the release exponent 'n'. The release exponent 'n' for HECR loaded phytosomes and simple HECR were 0.57 and 0.49, respectively. It has been reported, $0.45 \leq n$ relates to a Fickian diffusion mechanism for drug release, while $0.45 < n < 0.89$ to non-Fickian transport or anomalous transport mechanism. The n value of HECR loaded phytosomes and simple HECR are lower than 0.85 value indicating both diffusion and swelling controlled drug release kinetics of non Fickian or anomalous transport mechanism. The outcomes suggested HECR loaded phytosomes and Simple HECR follow an anomalous transport or non Fickian transport release mechanism governed by drug diffusion from the matrix as described by zero order for HECR loaded phytosomes and Higuchi model for Simple HECR, as shown in Table 4 and Fig. 8 for both nanovesicles formulations.

Hou *et al.* developed Mitomycin C soybean phosphatidylcholine complex, *in vitro* results reveal that the phytosomes complex displays 70 percent release over 8 h[42]. Whereas owing to another study published by Nandhini *et al.*, they developed vasaka phytosome, *in vitro* drug release analysis of vasaka phytosome demonstrated the sustained release characteristics of phytosome which reached 68.80 percent at 8 h[43]. Therefore, it has been proven that our medication release profile displays a superior release pattern as compared with previously reported data. Thus, *Cusucta reflexa* complexation with soya lecithin successfully improve the bioavailability.

3.11 Stability studies

The stability of any formulation during its shelf life is an important requirement, and to assure this, a stability study was performed. It was found that parameters studied for the stability study of phytosomal formulation, as shown in Table 5, were within limits. From the stability studies, it was confirmed that CR-phytosome did not show any characteristic changes in physical stability (Fig. 9). This indicates that the optimized formulations remained stable for 3 months.

4 Conclusion

Lipid-based vesicular carriers known as phytosomes can be utilized to carry plant-derived nutraceuticals like polyphenols. A novel phytosomal formulation of HECR was developed and *in vitro* evaluated to improve its oral bioavailability of polyphenol and flavonoids phytocompounds. The

Table 5 Stability analysis of the optimized phytosome formulation.

Months	Particle size (nm)	Entrapment efficiency (%)
0	173.5 ± 4.55	77.2 ± 2.77
1	178.9 ± 3.91	67.4 ± 8.29
2	184.7 ± 6.68	55.9 ± 3.60
3	196.5 ± 5.67	41.7 ± 7.34

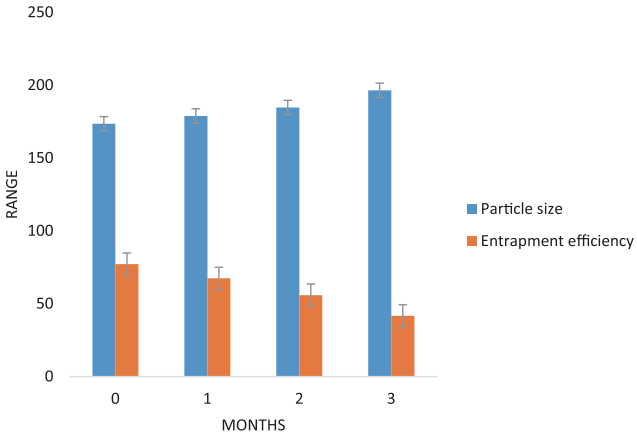

Fig. 9 Stability study for optimized batch.

complexation of soya lecithin with HECR phospholipids proved successful. The HECR loaded phytosomes have homogenous particle size distribution with smaller sizes. It is because of this that the phytosomes have increased permeability across the intestinal lipid barrier, which results in better bioavailability. To enhance the polyphenol and flavonoids phytocompounds' absorption, bioavailability, safety, and sustained drug release from extract, the study found an important role for phospholipids in the production of phytosomes with poor bioavailability phytocompounds. Furthermore, *in vitro* release tests showed that our suggested HECR-phytosomes released more polyphenol and flavonoids phytoconstituents than pure extract, confirming their improved permeability across the intestinal lipid membrane. This study's HECR-loaded phytosomes showed promising oral bioavailability. Thus, the delivery system shows better outcomes and successfully increased bioavailability of plant extract. As far as the authors know, there has never been any formulation using *Cuscuta reflexa* extract with phytosomes. The findings of this study could indicate that these systems could be considered potential prospects for the future delivery of active compounds from *Cuscuta reflexa* extracts. Moreover, using animal models in future studies will provide additional insight on the nanoformulation's efficacy *in vivo*.

Acknowledgments

This publication was supported by the Deanship of Scientific Research at Prince Sattam Bin Abdulaziz University Under the Research project No. 2021/03/18826.

Conflicts of Interest

The author declare no conflict of interest.

References

1) Direito, R.; Reis, C.; Roque, L.; Gonçalves, M.; Sanches-Silva, A. *et al.* Phytosomes with persimmon (*Diospyros kaki* L.) extract: Preparation and preliminary demonstration of *in vivo* tolerability. *Pharmaceutics* **11**, 296 (2019).
2) Tanruean, K.; Poolprasert, P.; Kumla, J.; Suwannarach, N.; Lumyong, S. Bioactive compounds content and their biological properties of acetone extract of *Cuscuta reflexa* Roxb. grown on various host plants. *Nat. Prod. Res.* **33**, 544-547 (2019).
3) Chatterjee, D.P.; Sahu, R.K.; Jha, A.K.; Dwivedi, J. Evaluation of antitumor activity of *Cuscuta reflexa* against Ehrlich ascites carcinoma in Swiss albino mice. *Trop. J. Pharm. Res.* **10**, 447-454 (2011).
4) Chatterjee, D.P.; Sahu, R.K.; Jha, A.K.; Dwivedi, J. Assessment of hepatoprotective activity of chloroform and ethanol extracts of whole plant of *Cuscuta reflexa* in CCl_4 treated rats and effectiveness of extracts on lipoprotein secretion by hepatic cells. *Pharmacologyonline* **3**, 799-809 (2010).
5) Shailajan, S.; Joshi, H.; Tiwari, B. A comparative estimation of quercetin content from *Cuscuta reflexa* Roxb. using validated HPTLC and HPLC techniques. *J. Appl. Pharm. Sci.* **4** (7), 123-128 (2014).
6) Zeeshan, S.; Zada, W.; Bhatti, H.A.; Abbas, G. *Cuscuta reflexa* L. & Roxb.: An implication of quercetin mediated monoamine oxidase inhibition in preclinical models of depression. *Hamdard Medicus* **59**, 5-11 (2016).
7) Chatterjee, D.P.; Sahu, R.K. Chemical characterization of the flavonoid constituents of *Cuscuta reflexa*. *UK J. Pharm. Biosci.* **2** (3), 13-16 (2014).
8) Muhammad, N.; Ullah, S.; Abu-Izneid, T.; Rauf, A.; Shehzad, O. *et al.* The pharmacological basis of *Cuscuta reflexa* whole plant as an antiemetic agent in pigeons. *Toxicol. Rep.* **7**, 1305-1310 (2020).
9) Direito, R.; Lima, A.; Rocha, J.; Ferreira, R.B.; Mota, J. *et al. Dyospiros kaki* phenolics inhibit colitis and colon cancer cell proliferation, but not gelatinase activities. *J. Nutr. Biochem.* **46**, 100-108 (2017).
10) Tan, B.L.; Norhaizan, M.E.; Liew, W.P.; Rahman, S.H. Antioxidant and oxidative stress: A mutual interplay in age-related diseases. *Front. Pharmacol.* **9**, 1162 (2018).
11) Anwar, E.; Farhana, N. Formulation and evaluation of phytosome-loaded maltodextrin-gum arabic microsphere system for delivery of *Camellia sinensis* extract. *J. Young Pharm.* **10** (2), s56-s62 (2018).
12) Riva, A.; Ronchi, M.; Petrangolini, G.; Bosisio, S.; Allegrini, P. Improved oral absorption of quercetin from quercetin phytosome®, a new delivery system based on food grade lecithin. *Eur. J. Drug Metab. Pharmacokinet.* **44**, 169-177 (2019).
13) Rich, G.T.; Buchweitz, M.; Winterbone, M.S.; Kroon, P.A.; Wilde, P.J. Towards an understanding of the low bioavailability of quercetin: a study of its interaction with intestinal lipids. *Nutrients* **9**, 111 (2017).
14) Bilia, A.R.; Isacchi, B.; Righeschi, C.; Guccione, C.; Bergonzi, M.C. Flavonoids loaded in nanocarriers: an opportunity to increase oral bioavailability and bioefficacy. *Food Nutr. Sci.* **5**, 1212-1227 (2014).
15) Sahu, R.K.; Aboulthana, W.M.; Mehta, D.K. Phytophospholipid complexation as a novel drug delivery system for management of cancer with better bioavailability: Current perspectives and future prospects. *Anti-Cancer Agents Med. Chem.* **21**, 1403-1412 (2021).
16) Detsi, A.; Kavetsou, E.; Kostopoulou, I.; Pitterou, I.; Pontillo, A. *et al.* Nanosystems for the encapsulation of natural products: The case of chitosan biopolymer as a matrix. *Pharmaceutics* **12**, 669 (2020).
17) Sayed, N.; Khurana, A.; Godugu, C. Pharmaceutical perspective on the translational hurdles of phytoconstituents and strategies to overcome. *J. Drug Deliv. Sci. Technol.* **53**, 101-201 (2019).
18) Salehi, B.; Machin, L.; Monzote, L.; Sharifi-Rad, J.; Ezzat, S.M. *et al.* Therapeutic potential of quercetin: New insights and perspectives for human health. *ACS Omega* **5**, 11849-11872 (2020).
19) Solnier, J.; Chang, C.; Roh, K.; Du, M.; Kuo, YC. *et al.* Quercetin lipomicel—A novel delivery system to enhance bioavailability of quercetin. *Journal of Natural Health Product Research* **3**, 1-8 (2021).
20) Biswas, S.; Mukherjee, P.K.; Kar, A.; Bannerjee, S.; Charoensub, R.; Duangyod, T. Optimized piperine–phospholipid complex with enhanced bioavailability and hepatoprotective activity. *Pharm. Dev. Technol.* **26** (1), 69-80 (2021).
21) Mishra, S.; Alhodieb, FS.; Barkat, MA.; Hassan, MZ.; Barkat, HA. *et al.* Antitumor and hepatoprotective effect of Cuscuta reflexa Roxb. in a murine model of colon cancer. *Pharm. Dev. Technol.* **2021**, 114597 (2021).
22) Liu, J.; Zou, S.; Liu, W.; Li, J.; Wang, H. *et al.* An established HPLC-MS/MS method for evaluation of the influence of salt processing on pharmacokinetics of six

compounds in cuscutae semen. *Molecules* **24**, 2502 (2019).
23) Upadhyay, K.; Gupta, N.K.; Dixit, V.K. Development and characterization of phyto-vesicles of β-sitosterol for the treatment of androgenetic alopecia. *Arch. Dermatol. Res.* **304**, 511-519(2012).
24) Ma, Y.Q.; Li, G.; Xu, J.H.; Zhang, J.; Zhang, Z.Z. *et al.* Combination of submicroemulsion and phospholipid complex for novel delivery of ursodeoxycholic acid. *Pharm. Dev. Technol.* **19**, 363-372(2014).
25) Singh, B.; Kapil, R.; Nandi, M.; Ahuja, N. Developing oral drug delivery systems using formulation by design: Vital precepts, retrospect and prospects. *Expert Opin. Drug Deliv.* **8**, 1341-1360(2011).
26) Anwar, E.; Farhana, N. Formulation and evaluation of phytosome-loaded maltodextrin-gum arabic microsphere system for delivery of *Camellia sinensis* extract. *J. Young Pharm.* **2**, 10(2018).
27) Yu, L.X.; Amidon, G.; Khan, M.A.; Hoag, S.W.; Polli, J. *et al.* Understanding pharmaceutical quality by design. *AAPS J.* **16**, 771-783(2014).
28) Mazumder, A.; Dwivedi, A.; Du Preez, J.L.; Du Plessis, J. *In vitro* wound healing and cytotoxic effects of sinigrin–phytosome complex. *Int. J. Pharm.* **498**, 283-293(2016).
29) Rasaee, S.; Ghanbarzadeh, S.; Mohammadi, M.; Hamishehkar, H. Nano phytosomes of quercetin: A promising formulation for fortification of food products with antioxidants. *Pharm. Sci.* **20**, 96-101(2014).
30) Karole, S.; Gupta, G.K. Preparation and evaluation of phytosomes containing ethanolic extract of leaves of Bombax ceiba for hepatoprotective activity. *Evaluation* **6**(2), 1-5(2019).
31) Sahu, A.R.; Bothara, S.B. Formulation and evaluation of phytosome drug delivery system of *Boswellia serrata* extract. *Int. J. Res. Med.* **4**(2), 94-99(2015).
32) Aung, T.T.; Xia, M.Y.; Hein, P.P.; Tang, R.; Zhang, D.D. *et al.* Chemical constituents from the whole plant of *Cuscuta reflexa*. *Nat. Prod. Bioprospect.* **10**, 337-344(2020).
33) Marasini, N.; Yan, Y.D.; Poudel, B.K.; Choi, H.G.; Yong, C.S.; Kim, J.O. Development and optimization of self-nanoemulsifying drug delivery system with enhanced bioavailability by Box–Behnken design and desirability function. *J. Pharm. Sci.* **101**, 4584-4596(2012).
34) Rathee, S.; Kamboj, A. Optimization and Development of Antidiabetic Phytosomes By Box-Benhken Design. *J. Liposome Res.* **28**, 161-172(2018).
35) Dubey, V.; Mishra, D.; Dutta, T.; Nahar, M.; Saraf, D.K.; Jain, N.K. Dermal and transdermal delivery of an anti-psoriatic agent via ethanolic liposomes. *J. Control. Release* **123**, 148-154(2007).
36) Ahmed, O.A.A.; Badr-Eldin, S.M. Development of an optimized avanafil-loaded invasomal transdermal film: *Ex vivo* skin permeation and *in vivo* evaluation. *Int. J. Pharm.* **570**, 118657(2019).
37) Bouarab, L.; Maherani, B.; Kheirolomoom, A.; Hasan, M.; Aliakbarian, B. *et al.* Influence of lecithin-lipid composition on physico-chemical properties of nanoliposomes loaded with a hydrophobic molecule. *Colloids Surf. B* **115**, 197-204(2014).
38) Maryana, W.; Rachmawati, H.; Mudhakir, D. Formation of phytosome containing silymarin using thin layer-hydration technique aimed for oral delivery. *Mater. Today Proc.* **2016**, 855-866(2016).
39) Tarlier, N.; Soulairol, I.; Sanchez-Ballester, N.; Baylac, G.; Aubert, A. *et al.* Deformation behavior of crystallized mannitol during compression using a rotary tablet press simulator. *Int. J. Pharm.* **547**, 142-149 (2018).
40) Putri, D.C.; Dwiastuti, R.; Marchaban, M.; Nugroho, A.K. Optimization of mixing temperature and sonication duration in liposome preparation. *J. Pharm. Sci. Commun.* **14**, 79-85(2017).
41) Danaei, M.; Dehghankhold, M.; Ataei, S.; Hasanzadeh, Davarani, F. *et al.* Impact of particle size and polydispersity index on the clinical applications of lipidic nanocarrier systems. *Pharmaceutics* **10**(2), 57 (2018).
42) Hou, Z.; Li, Y.; Huang, Y.; Zhou, C.; Lin, J. *et al.* Phytosomes loaded with mitomycin C-soybean phosphatidylcholine complex developed for drug delivery. *Mol. Pharm.* **10**, 90-101(2013).
43) Nandhini, S.; Ilango, K. Development and characterization of a nano-drug delivery system containing vasaka phospholipid complex to improve bioavailability using quality by design approach. *Res. Pharm. Sci.* **16**, 103 (2021).